Journal of Magnetic Resonance 204 (2010) 239–247

Contents lists available at ScienceDirect

Journal of Magnetic Resonance

journal homepage: www.elsevier.com/locate/jmr

Carbon-13 NOESY and equivalent protons: Methyl iodide dynamics

Dmytro Kotsyubynskyy [a], Jozef Kowalewski [a,*,1], Pekka Tallavaara [b], Ville-Veikko Telkki [b], Jukka Jokisaari [b,**], Evgeny Polyakov [a]

[a] Division of Physical Chemistry, Department of Materials and Environmental Chemistry, 10691 Stockholm University, Sweden
[b] NMR Research Group, Department of Physics, 90014 University of Oulu, Finland

ARTICLE INFO

Article history:
Received 8 February 2010
Revised 25 February 2010
Available online 6 March 2010

Keywords:
2D NOESY
Methyl iodide
J-coupled systems
Degenerate transitions
Dipole–dipole relaxation
Bloch–Wangsness–Redfield perturbation theory

ABSTRACT

We have shown that proton-coupled carbon-13 2D NOESY experiments, performed on degenerate spin systems, can provide unique quantitative information about anisotropic reorientational motions and molecular geometry. Relevant theory for AX_2 and AX_3 spin systems is presented, assuming the dipole–dipole and random field relaxation mechanisms of ^{13}C nucleus, and demonstrated on methyl iodide solution in chloroform. Agreement with experimental intensities of all the six independent peaks is very good in the whole range of mixing times (up to 45 s).

1. Introduction

Carbon-13 NMR relaxation measurements in solution are a powerful tool for studies of molecular dynamics in both small and large molecules. Spin–lattice (or longitudinal) relaxation is commonly studied under conditions of broadband proton irradiation [1,2]. Besides removing heteronuclear *J*-couplings, the decoupling renders the ^{13}C spin–lattice relaxation single exponential for the vast majority of cases [3]. Deviations from the single exponential spin-lattice relaxation occur if the proton spin systems contain degeneracies caused by the magnetic equivalence, e.g. in CH_2 and CH_3 groupings [4,5].

Studies of longitudinal carbon-13 relaxation without proton decoupling are much less common. Selected examples are given in references [6–18]. An important advantage of the study on *J*-coupled systems is that it allows investigations of cross-correlated relaxation phenomena, involving more than one rank-two interaction [19]. In certain situations, it may be advantageous to study the phenomena of this kind using two-dimensional techniques, such as different modifications of the NOESY scheme [20,21]. An interesting paper by Huang et al., published long time ago, proposed the use of carbon-13 as a "spy nucleus" in a 2D NOESY experiment, helping to map the population flows between various spin states of protons coupled to it [22]. Similar work, using small flip angle NOESY [23] extended this approach to homonuclear systems (without magnetic equivalence) and presented a more complete version of the theory [24]. In this communication, we extend the ^{13}C "spy nucleus" approach to systems with equivalent protons. We present the relevant theory and apply it to the example of ^{13}C-labelled methyl iodide in isotropic chloroform solution. We believe that similar approach can be applied to molecules dissolved in oriented systems, in particular for studying liquid crystalline solutions mixed with porous glass particles. Relevant studies are under way.

The dynamics of methyl iodide as a neat, isotropic liquid was studied intensively in the past by ^{13}C spin relaxation methods [25–29]. The molecule has a simple structure and axial symmetry (C_{3v} point group). Due to the small size, its reorientational motion in solution is very fast, especially around the symmetry axis, hence the spin-rotation relaxation mechanism is the most effective one. Next important mechanism, which has to be considered, is the ^{13}C–^{1}H dipole–dipole relaxation. Although Simcox et al. [29] have postulated that the ^{13}C chemical shielding anisotropy (CSA) mechanism is also non-negligible, we show that in our experimental conditions (chloroform solution at room temperature, magnetic field 4.7 T) the pure CSA relaxation is essentially non-observable. It was shown earlier, that other ^{13}C relaxation mechanisms, such as the ^{13}C–^{127}I dipole–dipole and the scalar

* Corresponding author.
** Corresponding author.
E-mail addresses: Jozef.Kowalewski@mmk.su.se (J. Kowalewski), Jukka.Jokisaari@oulu.fi (J. Jokisaari).
[1] Principal corresponding author.

1090-7807/$ - see front matter © 2010 Elsevier Inc. All rights reserved.
doi:10.1016/j.jmr.2010.03.003

relaxation of the second kind (in the terminology of Abragam [30]) contribute very little to the overall relaxation rate [25–29]. Attempts were also made to explain the magnitudes of relaxation rates and molecular reorientation rates, and their temperature dependence [26,28,29].

In the present study, we use NOESY experiments as the main source of relaxation data. We consider two relaxation mechanisms: the spin-rotation interaction, treated phenomenologically as a random field process, and all the dipole–dipole interactions among the four spins. As shown by Huang et al. [22] and Oschkinat et al. [24], there is a correspondence between the signal intensities in proton-coupled ^{13}C NOESY spectra and the relaxation matrix elements. It is possible to obtain transition probabilities, containing the dynamic information, within the initial rate approximation [22]. Alternatively, one can solve the master differential equation for energy level populations [24]. When the protons are magnetically-equivalent and the symmetry of the system is high, as is the case in the CH_3I molecule, then some energy levels become degenerate and the Redfield formalism [31] must be used instead of the simple transition probabilities theory [5,10,32]. We therefore aim at utilizing a modification of the method of Oschkinat et al. [24] for the methyl iodide case applying simultaneous fitting of the whole pattern of signals occurring in the NOESY spectra (all measured intensities of diagonal and off-diagonal signals) obtained with different mixing times. Equations for the relaxation matrix elements, expressed in a minimal operator basis set suitable for the NOESY experiments, are provided for fully degenerate CH_2 and CH_3 spin systems under the assumption of negligible CSA relaxation (see further text).

It is shown that such an approach allows for accurate determination of reorientational parameters for methyl iodide in isotropic solution, assuming symmetrical top diffusional model [2,5,33].

2. Theory

2.1. General

Molecular motions manifest themselves in spectral densities and can be observed as nuclear spin relaxation effects [2,30,34–36]. Usually experiments leading to the determination of spin-lattice (R_1) and spin–spin (R_2) relaxation rates as well as the heteronuclear NOE parameter are used as a source of information, sometimes together with different cross-correlated relaxation rates (CCRRs) [16,19]. All of those are in fact linear combinations of spectral densities and do not provide much unique information in the extreme narrowing regime. Moreover, cross-correlated rates are usually determined within the initial rate approximation [16,19], and thus have a higher uncertainty than the R_1 and R_2 rates. As an alternative, 2D NOESY (EXSY) experiments can be a useful source of information concerning molecular motions without the use of the concept of R_1, R_2, and so on, but operating directly on the relaxation matrix elements. The spin-diffusion effect, which can disturb measurements, does not occur in the case of methyl iodide in solution, because the four spin system is well-defined (the ^{127}I spin can be safely neglected due to its small relaxation effect) and the studied solution is not concentrated. It is therefore possible to analyze accurately the dependence of intensities of all the diagonal and off-diagonal signals on the mixing time, avoiding the initial rate approximation and possible errors originating from it.

The statistical state of a spin system is described by the density operator or the density matrix ρ [2,30,31]. In accordance with the Bloch–Wangsness–Redfield perturbation theory [31,37], the differential equation for the elements of the density matrix $\tilde{\rho}$ (the tilde denotes the interaction representation) can be written as:

$$\frac{d\tilde{\rho}_{\alpha\alpha'}(t)}{dt} = \sum_{\beta\beta'} e^{i(\alpha-\alpha'-\beta+\beta')t} R_{\alpha\alpha'\beta\beta'} \tilde{\rho}_{\beta\beta'}(t) \tag{1}$$

where α, α', β, and β' denote all possible eigenstates of the considered spin system, and the terms inside the exponent are written in short instead of $\omega_\alpha - \omega_{\alpha'} - \omega_\beta + \omega_{\beta'}$. Here, we use the direct product states basis because of its simplicity and clear physical meaning. $\tilde{\rho}(t)$ is a column vector of the density matrix elements (whose time dependence will be omitted in the notation from now on), and $R_{\alpha\alpha'\beta\beta'}$ is a *relaxation matrix* element given by Eq. (3). The expectation value of any observable Q, corresponding to the operator $\widehat{Q}$, at the time t can be obtained from the density matrix using Eq. (2), where both $\widehat{Q}$ and $\tilde{\rho}$ are given in the form of matrix representations. In other words, Q can be presented as a linear combination of the elements of $\tilde{\rho}$.

$$\langle Q(t)\rangle = Tr\left[\widehat{Q}\tilde{\rho}(t)\right] \tag{2}$$

It follows from Eq. (1) that, for a system having n energy states, the dimension of the density matrix will be $n \times n$, and the same (n^2) will be the length of the $\tilde{\rho}_{ij}$ vector in the Liouville space. Consequently, the R matrix will have a dimension of $n^2 \times n^2$. Usually, however, the *secular approximation* is applied, implying retaining only those elements of R, for which $\omega_\alpha - \omega_{\alpha'} - \omega_\beta + \omega_{\beta'} = 0$ [2,31]. Elements of the R matrix are given by:

$$R_{\alpha\alpha'\beta\beta'} = \frac{1}{2}\left(J_{\alpha\beta\alpha'\beta'}(\alpha'-\beta') + J_{\alpha\beta\alpha'\beta'}(\alpha-\beta) - \delta_{\alpha'\beta'}\sum_\gamma J_{\gamma\beta\gamma\alpha}(\gamma-\beta) - \delta_{\alpha\beta}\sum_\gamma J_{\gamma\alpha'\gamma\beta'}(\gamma-\beta')\right) \tag{3}$$

where $J_{\alpha\alpha'\beta\beta'}(\omega)$ elements are given by:

$$J_{\alpha\alpha'\beta\beta'}(\omega) = \sum_\eta \sum_{\eta'} \xi_\eta \xi_{\eta'} \sum_{q=-l}^{l} \langle\alpha|\widehat{T}^{\eta}_{l,-q}|\alpha'\rangle\langle\beta'|\widehat{T}^{*\eta'}_{l,-q'}|\beta\rangle J_l^{\eta\eta'}(\omega) \tag{4}$$

The operators relevant in the proton-coupled ^{13}C NOESY experiments are associated with the spin–lattice (longitudinal) relaxation processes, and can be represented conveniently using single transition operators introduced by Wokaun and Ernst [38] (see the section devoted to the methylene group). The matrix representations of these operators have only diagonal elements different from zero, therefore according to Eq. (2) we are interested just in the diagonal elements of the density matrix. However, due to the degeneracy of some energy levels in the AX_n spin systems ($n > 1$), condition $\omega_\alpha - \omega_{\alpha'} - \omega_\beta + \omega_{\beta'} = 0$ is fulfilled as well for some off-diagonal elements of density matrix. Therefore those also need to be included [10,32].

In Eq. (4), ξ_i denotes the interaction strength, e.g. the dipole–dipole coupling constant in the case of dipolar interaction, $\widehat{T}^i_{l,-q}$ is the q-th component of the rank-l irreducible tensor operator, dependent only on spin operators, and $J_l^{\eta\eta'}(\omega)$ is a reduced spectral density function of rank l corresponding to interactions η and η'. The summation over η and η' goes through all the possible interactions; thus, all the cross-correlations are accounted for in a natural way. Interaction strength constants may be incorporated into $J_l^{\eta\eta'}(\omega)$, forming "complete" (non-reduced) spectral densities, which facilitates the notation.

After constructing the relaxation matrix using Eqs. (3) and (4), there are two ways to proceed to the final result. The first one implies that Eq. (1) will be solved directly, using linear algebra methods, and then converted into observables through a matrix which

transforms populations to/from coherences. This approach is straightforward and convenient when the spin system does not contain degenerate transitions [8]. In this case, the matrix S with elements corresponding to the intensities in the proton-coupled NOESY spectra will be given by (assuming weak coupling conditions) [24]:

$$S_{M\times M} = P_{M\times N} U_R \exp\left(-U_R^{-1} R_{N\times N} U_R \tau_m\right) U_R^{-1} P_{N\times M} \tag{5}$$

where U_R is the matrix of column eigenvectors of R, τ_m is the mixing time, the rectangular matrix $P_{N\times M}$ converts coherences into populations, and $P_{M\times N} = P_{N\times M}^T$ does the opposite conversion [24].

The second way is to set up the relaxation matrix using a new, smaller and orthogonal basis set, which will contain the observables in the NOESY experiment. The relaxation matrix in this basis set will be denoted as A, and the matrix formed by column vectors representing the basis vectors as V. We start with V containing vectors corresponding to the NOESY observables. These vectors span a subspace K of the space of all the observables. Now, the problem is that this basis is incomplete with respect to dynamics defined by the relaxation matrix R. Since R in general couples all the observables, an initial state within K will during time evolution acquire components outside of K. Thus, we have to find invariant subspace L, containing K, such that any vector belonging to L will not leave it during evolution under R [39]. As will be shown below, the dimension of L is in practice not much greater than that of K.

The practical procedure of determining the remaining basis vectors to make V complete under dynamical evolution is the following: first we define the matrix B as:

$$B = \left(1 - VV^T\right)RV \tag{6}$$

The matrix B contains components of RV, orthogonal to the space spanned by the basis vectors V. Therefore, if the basis set V is complete, B will be a zero matrix, and if it is not, some non-zero elements will be present. Vectors needed for completion of the basis set can be guessed from the symmetries of the column(s) of the matrix B. Then we proceed in an iterative way, adding one or few vectors to the V and recomputing B each time. One has to be aware that the described procedure may lead to a basis set which is not minimal, so additional checks are advised.

The bases obtained for AX_2 and AX_3 spin systems are similar (in part identical) to the bases reported by Werbelow and Grant [10]. Among the advantages of the described method are: a direct correspondence of a part of the matrix to the experimental spectrum, and (usually) the reduction of the dimension of the problem. The transformation of R into A is simple, and if the V vectors are normalized to 1, A will be a square symmetric matrix, with dimensions equal to the number of basis vectors:

$$A = V^T RV \tag{7}$$

The final solution of the problem will be similar to Eq. (5), but now the matrix A will replace R, and, if 90° pulses in the NOESY sequence are used, the P matrices will have just few non-zero elements corresponding to population deviations from the thermal equilibrium at the beginning of the mixing period:

$$S = P_A^T U_A \exp\left(-U_A^{-1}\left(V^T RV\right)U_A \tau_m\right) U_A^{-1} P_A \tag{8}$$

Here, the P_A matrix contains square roots of number of transitions, corresponding to the certain observable, on its diagonal, while all non-diagonal elements are zero, its main purpose is to provide correct relative magnitudes of the elements of the matrix S. For example, the P_A matrix for the AX_3 spin system will have dimensions 11 by 4, and only 4 non-zero elements:

$$P_A = \begin{bmatrix} 1 & 0 & 0 & 0 \\ 0 & \sqrt{3} & 0 & 0 \\ 0 & 0 & \sqrt{3} & 0 \\ 0 & 0 & 0 & 1 \\ 0 & 0 & 0 & 0 \\ \vdots & \vdots & \vdots & \vdots \\ 0 & 0 & 0 & 0 \end{bmatrix} \tag{9}$$

The resulting elements of the matrix S for a certain τ_m value will be proportional to the intensities of the measured NOESY spectrum with a one-to-one correspondence.

Let us now discuss practical aspects of the calculations. The matrix R and the basis vectors V can be obtained either analytically, for example, using computer algebra software, or by calculating elements of the R matrix "on the fly", in both cases according to Eqs. (3) and (4). The analytical solution seems to be more useful, because once the elements of the A matrix are calculated, Eqs. (3) and (4) are no longer needed, it might also be helpful for comparison of the results. Mature programs capable to calculate a symbolic form of relaxation matrix elements or a relaxation rate corresponding to a given operator are already available for free use [40,41]. We have, however, written our own script using Maxima [42], which is intended to compute elements of the relaxation matrix for spin systems with possible degeneracies. The correctness of the outcome produced by the script was verified by comparison with the results for AX_2 and AX_3 spin systems published by Werbelow and Grant [10], and a complete equivalence of the two approaches was found. This comparison required transformation of the R using basis sets given by those authors, according to Eq. (7).

2.2. Basis vectors and relaxation matrices for the methylene group

The energy level diagram for the CH_2 group, analogous to that of Werbelow and Grant [10], is shown in Fig. 1. We use the same notation and the same set of direct product states as the basis:

$$\begin{aligned} |1\rangle = |\alpha\alpha\alpha\rangle, \quad |2\rangle = |\beta\alpha\alpha\rangle, \quad |3\rangle = |\alpha\alpha\beta\rangle, \quad |4\rangle = |\alpha\beta\alpha\rangle, \quad |5\rangle \\ = |\beta\alpha\beta\rangle = \lambda|4\rangle, \quad |6\rangle = |\beta\beta\alpha\rangle = \lambda|3\rangle, \quad |7\rangle = |\alpha\beta\beta\rangle \\ = \lambda|2\rangle, \quad |8\rangle = |\beta\beta\beta\rangle = \lambda|1\rangle \end{aligned} \tag{10}$$

where λ stands for total spin inversion operator. The first spin is the carbon-13.

The pairs of levels 3, 4, and 5, 6 are degenerate, and the secular approximations makes it necessary to consider 4 off-diagonal ele-

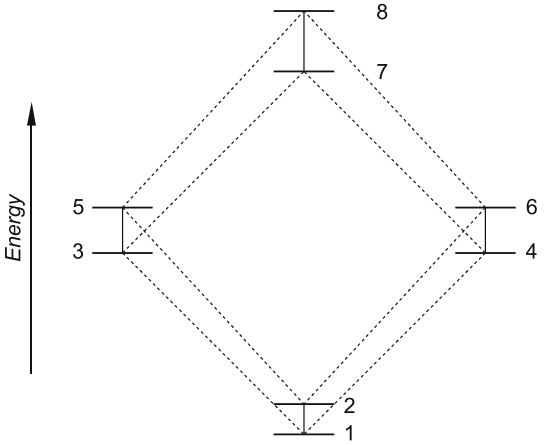

Fig. 1. Energy level diagram for the $^{13}CH_2$ group. Single quantum carbon and proton transitions are indicated with solid and dashed lines, respectively.

ments of the density matrix: $\rho_{3,4}$, $\rho_{4,3}$, $\rho_{5,6}$, $\rho_{6,5}$ (from here on, we omit the tilde to simplify the notation) in addition to the diagonal ones. The complete orthogonal basis set relevant for the NOESY experiment is then given by the following vectors consisting of the density matrix elements $\rho_{i,j}$:

$$
\begin{aligned}
V_1 &= \rho_{1,1} - \rho_{2,2}\\
V_2 &= \frac{1}{\sqrt{2}}(\rho_{3,3} + \rho_{4,4} - \rho_{5,5} - \rho_{6,6})\\
V_3 &= \rho_{7,7} - \rho_{8,8}\\
V_4 &= \frac{1}{\sqrt{2}}(\rho_{1,1} + \rho_{2,2} - \rho_{7,7} - \rho_{8,8})\\
V_5 &= \frac{1}{2}(\rho_{1,1} + \rho_{2,2} - \rho_{3,3} - \rho_{4,4} - \rho_{5,5} - \rho_{6,6} + \rho_{7,7} + \rho_{8,8})\\
V_6 &= \frac{1}{\sqrt{2}}(\rho_{3,4} + \rho_{4,3} + \rho_{5,6} + \rho_{6,5})\\
V_7 &= \frac{1}{\sqrt{2}}(\rho_{3,4} + \rho_{4,3} - \rho_{5,6} - \rho_{6,5})
\end{aligned}
\tag{11}
$$

The first three vectors correspond to observables of the NOESY spectrum. Those can be presented using single transition operators:

$$
\begin{aligned}
V_1 &= Tr\left[I_z^{(1,2)}\rho\right]\\
V_2 &= \frac{1}{\sqrt{2}}Tr\left[(I_z^{(3,5)} + I_z^{(4,6)})\rho\right]\\
V_3 &= Tr\left[I_z^{(7,8)}\rho\right]
\end{aligned}
\tag{12}
$$

where for ψ_i and ψ_j being eigenstates of the spin system [38]:

$$
\langle\psi_i|I_z^{(r,s)}|\psi_j\rangle = \frac{1}{2}(\delta_{ir}\delta_{jr} - \delta_{is}\delta_{js}) \tag{13}
$$

The remaining 4 vectors (V_4–V_7) are needed to complete the basis set. Two of them (V_4, V_5) contain solely the diagonal elements of the density matrix ρ, and the last two only the off-diagonal elements. The last 4 vectors are identical to those found by Werbelow and Grant. However, they correspond to the basis vectors belonging to the two orthogonal basis sets, y and q, having 4 and 3 elements, respectively [10]: $V_4 \equiv y_1$, $V_5 \equiv q_2$, $V_6 \equiv q_3$, $V_7 \equiv y_4$. The "mixing" of the basis vectors is a consequence of reduced symmetry of our basis set vectors in comparison with those defined in Ref. [10].

Utilizing Eq. (7), the elements of the A matrix can be given as:

$$
\begin{aligned}
A_{1,1} &= \frac{1}{2}A_{5,5} + 2J_{HH}(2\omega_H) + 2J_{HCH}(\omega_C) + 2J_{CH}(\omega_C) + rf_C\\
A_{1,2} &= \frac{1}{\sqrt{2}}(2J_{CH}(\omega_H + \omega_C) + \frac{1}{3}J_{CH}(\omega_H - \omega_C) - J_{HH}(\omega_H)\\
&\quad - J_{CH}(\omega_H) - rf_H)\\
A_{1,3} &= -2J_{HH}(2\omega_H)\\
A_{1,4} &= \sqrt{2}\left(J_{CH}(\omega_H + \omega_C) - \frac{1}{6}J_{CH}(\omega_H - \omega_C) + J_{CHH}(\omega_H)\right),\\
A_{1,5} &= \sqrt{2}A_{1,4}\\
A_{1,6} &= -\sqrt{2}\left(J_{HCH}(\omega_H + \omega_C) - \frac{1}{6}J_{HCH}(\omega_H - \omega_C) + J_{CHH}(\omega_H)\right)\\
A_{1,7} &= \frac{1}{\sqrt{2}}(2J_{HCH}(\omega_H + \omega_C) + \frac{1}{3}J_{HCH}(\omega_H - \omega_C) - J_{HH}(\omega_H)\\
&\quad - J_{HCH}(\omega_H) - rf_H)\\
A_{2,2} &= \frac{1}{2}A_{5,5} - 2J_{HCH}(\omega_C) + 2J_{CH}(\omega_C) + rf_C, \quad A_{2,3} = A_{1,2}\\
A_{2,4} &= 2J_{CH}(\omega_H + \omega_C) - \frac{1}{3}J_{CH}(\omega_H - \omega_C) - 2J_{CHH}(\omega_H)\\
A_{2,5} &= 0, \quad A_{2,6} = 0\\
A_{2,7} &= 2J_{HCH}(\omega_H + \omega_C) + \frac{1}{3}J_{HCH}(\omega_H - \omega_C) + J_{HH}(\omega_H)\\
&\quad + J_{HCH}(\omega_H) + rf_H\\
A_{3,3} &= A_{1,1}, \quad A_{3,4} = A_{1,4}, \quad A_{3,5} = -A_{1,5}, \quad A_{3,6} = -A_{1,6},\\
A_{3,7} &= A_{1,7}\\
A_{4,4} &= \frac{1}{2}A_{5,5} + 4J_{HH}(2\omega_H)\\
A_{4,5} &= 0, \quad A_{4,6} = 0\\
A_{4,7} &= 2J_{HCH}(\omega_H + \omega_C) - \frac{1}{3}J_{HCH}(\omega_H - \omega_C) - 2J_{CHH}(\omega_H)\\
A_{5,5} &= 2(2J_{CH}(\omega_H + \omega_C) + \frac{1}{3}J_{CH}(\omega_H - \omega_C) + J_{HH}(\omega_H)\\
&\quad + J_{CH}(\omega_H) + rf_H)\\
A_{5,6} &= -\sqrt{2}A_{2,7}, \quad A_{5,7} = 0\\
A_{6,6} &= \frac{1}{2}A_{5,5} - 2J_{HCH}(\omega_C) + 2J_{CH}(\omega_C) - \frac{4}{3}J_{HCH}(0) + \frac{4}{3}J_{CH}(0)\\
A_{6,7} &= 0, \quad A_{7,7} = \frac{1}{2}A_{5,5} + rf_C - \frac{4}{3}J_{HCH}(0) + \frac{4}{3}J_{CH}(0)
\end{aligned}
\tag{14}
$$

Some A matrix elements are expressed *via* element $A_{5,5}$ to shorten the formulas. Here and later we employ the same normalization of spectral densities as in Ref. [10]. The spectral densities of type J_{HH} and J_{CH} are of the "auto" type, and those containing three or four (for four-spins system) atomic symbols are cross-correlated ones. In case of three atomic symbols the middle one is common for both interactions.

We retain the frequencies at which the J's are to be evaluated, even though we are in extreme narrowing range and it is strictly speaking not necessary. The symbols rf_H and rf_C denote the random field type rates, which in our treatment are just fitting parameters. Analytical equations for spectral densities for AX_3 spin system will be given in the next section.

It should be stressed that the present treatment is valid for $^{13}CH_2$ groups with magnetically-equivalent protons. The common case of methylene groups with the carbon-13 spectrum in the form of a triplet but with the two protons characterized by different chemical shifts requires, strictly speaking, a somewhat different treatment. Typically, such groupings are either approximated as AX_2 [12] or AMX [16].

2.3. Basis vectors and relaxation matrices for the methyl group

The formation of a complete orthogonal basis set for the *methyl* group is more challenging than that of a methylene group, because there are 40 non-zero elements in the density matrix. The procedure is essentially the same as described above. Again, we use the numbering of the basis product states following Werbelow and Grant [10]. For the eigenstates defined in Eq. (15) (the first spin denotes carbon-13) the groups of levels 3, 4, 5; 6, 7, 8; 9, 10, 11; and 12, 13, 14 are degenerate. The energy level diagram for the methyl group, again based on the work of Werbelow and Grant [10] is shown in Fig. 2.

$$
\begin{aligned}
|1\rangle &= |\alpha\alpha\alpha\alpha\rangle, \quad |2\rangle = |\beta\alpha\alpha\alpha\rangle, \quad |3\rangle = |\alpha\alpha\alpha\beta\rangle, \quad |4\rangle\\
&= |\alpha\alpha\beta\alpha\rangle, \quad |5\rangle = |\alpha\beta\alpha\alpha\rangle, \quad |6\rangle = |\beta\alpha\alpha\beta\rangle, \quad |7\rangle\\
&= |\beta\alpha\beta\alpha\rangle, \quad |8\rangle = |\beta\beta\alpha\alpha\rangle, \quad |9\rangle = |\alpha\alpha\beta\beta\rangle = \lambda|8\rangle, \quad |10\rangle\\
&= |\alpha\beta\alpha\beta\rangle = \lambda|7\rangle, \quad |11\rangle = |\alpha\beta\beta\alpha\rangle = \lambda|6\rangle, \quad |12\rangle = |\beta\alpha\beta\beta\rangle\\
&= \lambda|5\rangle, \quad |13\rangle = |\beta\beta\alpha\beta\rangle = \lambda|4\rangle, \quad |14\rangle = |\beta\beta\beta\alpha\rangle\\
&= \lambda|3\rangle, \quad |15\rangle = |\alpha\beta\beta\beta\rangle = \lambda|2\rangle, \quad |16\rangle = |\beta\beta\beta\beta\rangle = \lambda|1\rangle
\end{aligned}
\tag{15}
$$

Therefore, we need this time to consider 24 off-diagonal elements. In the case of a methyl group there are four signals (observables) on the diagonal in the NOESY spectrum, and additional 7

vectors are needed to complete the basis. Three of them contain just the diagonal elements of ρ, and the rest only the off-diagonal ones.

The normalized basis vectors are given by:

$$
\begin{aligned}
V_1 &= \rho_{1,1} - \rho_{2,2}\\
V_2 &= \frac{1}{\sqrt{3}}(\rho_{3,3} + \rho_{4,4} + \rho_{5,5} - \rho_{6,6} - \rho_{7,7} - \rho_{8,8})\\
V_3 &= \frac{1}{\sqrt{3}}(\rho_{9,9} + \rho_{10,10} + \rho_{11,11} - \rho_{12,12} - \rho_{13,13} - \rho_{14,14})\\
V_4 &= \rho_{15,15} - \rho_{16,16}\\
V_5 &= \frac{1}{\sqrt{2}}(\rho_{1,1} + \rho_{2,2} - \rho_{15,15} - \rho_{16,16})\\
V_6 &= \frac{1}{\sqrt{6}}(\rho_{3,3} + \rho_{4,4} + \rho_{5,5} + \rho_{6,6} + \rho_{7,7} + \rho_{8,8}\\
&\quad - \rho_{9,9} - \rho_{10,10} - \rho_{11,11} - \rho_{12,12} - \rho_{13,13} - \rho_{14,14})\\
V_7 &= \frac{1}{2\sqrt{6}}(-3\rho_{1,1} - 3\rho_{2,2} + \rho_{3,3} + \rho_{4,4} + \rho_{5,5} + \rho_{6,6}\\
&\quad + \rho_{7,7} + \rho_{8,8} + \rho_{9,9} + \rho_{10,10} + \rho_{11,11} + \rho_{12,12}\\
&\quad + \rho_{13,13} + \rho_{14,14} - 3\rho_{15,15} - 3\rho_{16,16})\\
V_8 &= \frac{1}{\sqrt{6}}(\rho_{3,4} + \rho_{3,5} + \rho_{4,3} + \rho_{4,5} + \rho_{5,3} + \rho_{5,4}\\
&\quad - \rho_{12,13} - \rho_{12,14} - \rho_{13,12} - \rho_{13,14} - \rho_{14,12} - \rho_{14,13})\\
V_9 &= \frac{1}{\sqrt{6}}(\rho_{3,4} + \rho_{3,5} + \rho_{4,3} + \rho_{4,5} + \rho_{5,3} + \rho_{5,4}\\
&\quad + \rho_{12,13} + \rho_{12,14} + \rho_{13,12} + \rho_{13,14} + \rho_{14,12} + \rho_{14,13})\\
V_{10} &= \frac{1}{\sqrt{6}}(\rho_{6,7} + \rho_{6,8} + \rho_{7,6} + \rho_{7,8} + \rho_{8,6} + \rho_{8,7}\\
&\quad - \rho_{9,10} - \rho_{9,11} - \rho_{10,9} - \rho_{10,11} - \rho_{11,9} - \rho_{11,10})\\
V_{11} &= \frac{1}{\sqrt{6}}(\rho_{6,7} + \rho_{6,8} + \rho_{7,6} + \rho_{7,8} + \rho_{8,6} + \rho_{8,7}\\
&\quad + \rho_{9,10} + \rho_{9,11} + \rho_{10,9} + \rho_{10,11} + \rho_{11,9} + \rho_{11,10})
\end{aligned}
\tag{16}
$$

The relaxation matrix elements in this new basis set are:

$$
\begin{aligned}
A_{1,1} &= A_{5,5} + 6J_{\mathrm{HCH}}(\omega_{\mathrm{C}}) + 3J_{\mathrm{CH}}(\omega_{\mathrm{C}}) + rf_{\mathrm{C}}\\
A_{1,2} &= \sqrt{3}(J_{\mathrm{CH}}(\omega_{\mathrm{H}} + \omega_{\mathrm{C}}) + \frac{1}{6}J_{\mathrm{CH}}(\omega_{\mathrm{H}} - \omega_{\mathrm{C}}) - J_{\mathrm{HHH}}(\omega_{\mathrm{H}}) - J_{\mathrm{HH}}(\omega_{\mathrm{H}})\\
&\quad - \frac{1}{2}J_{\mathrm{CH}}(\omega_{\mathrm{H}}) - \frac{1}{2}rf_{\mathrm{H}})\\
A_{1,3} &= -2\sqrt{3}J_{\mathrm{HH}}(2\omega_{\mathrm{H}}), \quad A_{1,4} = 0\\
A_{1,5} &= \frac{1}{\sqrt{2}}\left(3J_{\mathrm{CH}}(\omega_{\mathrm{H}} + \omega_{\mathrm{C}}) - \frac{1}{2}J_{\mathrm{CH}}(\omega_{\mathrm{H}} - \omega_{\mathrm{C}}) + 6J_{\mathrm{CHH}}(\omega_{\mathrm{H}})\right)\\
A_{1,6} &= -\frac{1}{\sqrt{3}}A_{1,5}, \quad A_{1,7} = -\frac{2}{\sqrt{3}}A_{1,5}
\end{aligned}
$$

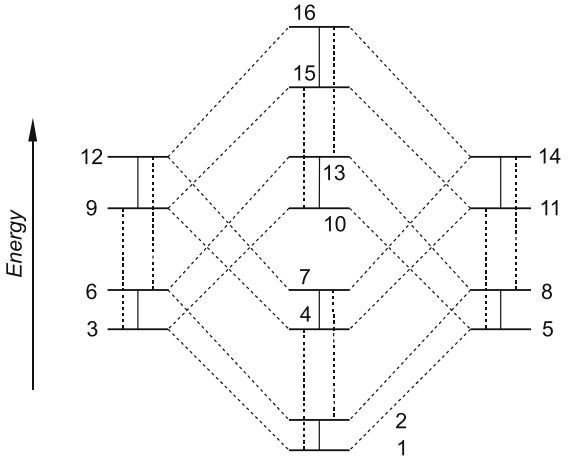

Fig. 2. Energy level diagram for the $^{13}CH_3$ group. Single quantum carbon and proton transitions are indicated with solid and dashed lines, respectively.

$$
\begin{aligned}
A_{1,8} &= \sqrt{\frac{3}{2}}\left(\frac{1}{3}J_{\mathrm{HCH}}(\omega_{\mathrm{H}} - \omega_{\mathrm{C}}) - 2J_{\mathrm{HHH}}(2\omega_{\mathrm{H}}) - \frac{3}{2}J_{\mathrm{HHH}}(\omega_{\mathrm{H}}) - \frac{1}{2}J_{\mathrm{HH}}(\omega_{\mathrm{H}})\right.\\
&\quad \left. - \frac{1}{2}J_{\mathrm{HCH}}(\omega_{\mathrm{H}}) - J_{\mathrm{CHHH}}(\omega_{\mathrm{H}}) - J_{\mathrm{CHH}}(\omega_{\mathrm{H}}) - \frac{1}{2}rf_{\mathrm{H}}\right)\\
A_{1,9} &= A_{1,8} + 2\sqrt{6}J_{\mathrm{HHH}}(2\omega_{\mathrm{H}})\\
A_{1,10} &= -A_{1,8} - \sqrt{6}\left(J_{\mathrm{HCH}}(\omega_{\mathrm{H}} + \omega_{\mathrm{C}}) - \frac{1}{6}J_{\mathrm{HCH}}(\omega_{\mathrm{H}} - \omega_{\mathrm{C}}) + J_{\mathrm{CHHH}}(\omega_{\mathrm{H}}) + J_{\mathrm{CHH}}(\omega_{\mathrm{H}})\right)\\
A_{1,11} &= A_{1,10} - 2\sqrt{6}J_{\mathrm{HHH}}(2\omega_{\mathrm{H}})\\
A_{2,2} &= A_{1,1} - 4J_{\mathrm{HH}}(2\omega_{\mathrm{H}}) - 4J_{\mathrm{HHH}}(\omega_{\mathrm{H}}) - 8J_{\mathrm{HCH}}(\omega_{\mathrm{C}})\\
A_{2,3} &= \frac{2}{\sqrt{3}}A_{1,2} + 4J_{\mathrm{HHH}}(\omega_{\mathrm{H}}), \quad A_{2,4} = A_{1,3}\\
A_{2,5} &= \sqrt{6}\left(\frac{1}{2}J_{\mathrm{CH}}(\omega_{\mathrm{H}} + \omega_{\mathrm{C}}) - \frac{1}{12}J_{\mathrm{CH}}(\omega_{\mathrm{H}} - \omega_{\mathrm{C}}) - J_{\mathrm{CHH}}(\omega_{\mathrm{H}})\right)\\
A_{2,6} &= \sqrt{2}\left(\frac{3}{2}J_{\mathrm{CH}}(\omega_{\mathrm{H}} + \omega_{\mathrm{C}}) - \frac{1}{4}J_{\mathrm{CH}}(\omega_{\mathrm{H}} - \omega_{\mathrm{C}}) + J_{\mathrm{CHH}}(\omega_{\mathrm{H}})\right)\\
A_{2,7} &= -\frac{2}{\sqrt{3}}A_{2,5}, \quad A_{2,8} = -\frac{1}{\sqrt{3}}A_{1,8} + \sqrt{2}\left(2J_{\mathrm{HCH}}(\omega_{\mathrm{H}} + \omega_{\mathrm{C}}) + \frac{1}{3}J_{\mathrm{HCH}}(\omega_{\mathrm{H}} - \omega_{\mathrm{C}})\right)\\
A_{2,9} &= \frac{1}{\sqrt{2}}\left(\frac{1}{3}J_{\mathrm{HCH}}(\omega_{\mathrm{H}} - \omega_{\mathrm{C}}) + 2J_{\mathrm{HHH}}(2\omega_{\mathrm{H}}) + \frac{1}{2}J_{\mathrm{HHH}}(\omega_{\mathrm{H}}) + \frac{3}{2}J_{\mathrm{HH}}(\omega_{\mathrm{H}})\right.\\
&\quad \left. + \frac{3}{2}J_{\mathrm{HCH}}(\omega_{\mathrm{H}}) + 3J_{\mathrm{CHHH}}(\omega_{\mathrm{H}}) - J_{\mathrm{CHH}}(\omega_{\mathrm{H}}) + \frac{3}{2}rf_{\mathrm{H}}\right)\\
A_{2,10} &= -\frac{1}{\sqrt{3}}A_{1,10} - \sqrt{2}\left(2J_{\mathrm{HCH}}(\omega_{\mathrm{H}} + \omega_{\mathrm{C}}) + \frac{1}{3}J_{\mathrm{HCH}}(\omega_{\mathrm{H}} - \omega_{\mathrm{C}})\right)\\
A_{2,11} &= -A_{2,9} - \sqrt{2}\left(J_{\mathrm{HCH}}(\omega_{\mathrm{H}} + \omega_{\mathrm{C}}) - \frac{1}{6}J_{\mathrm{HCH}}(\omega_{\mathrm{H}} - \omega_{\mathrm{C}}) - 3J_{\mathrm{CHHH}}(\omega_{\mathrm{H}}) + J_{\mathrm{CHH}}(\omega_{\mathrm{H}})\right)\\
A_{3,3} &= A_{2,2}, \quad A_{3,4} = A_{1,2}, \quad A_{3,5} = A_{2,5}, \quad A_{3,6} = A_{2,6}\\
A_{3,7} &= -A_{2,7}, \quad A_{3,8} = A_{2,8}, \quad A_{3,9} = -A_{2,9}, \quad A_{3,10} = A_{2,10}\\
A_{3,11} &= -A_{2,11}, \quad A_{4,4} = A_{1,1}, \quad A_{4,5} = A_{1,5}, \quad A_{4,6} = A_{1,6}\\
A_{4,7} &= -A_{1,7}, \quad A_{4,8} = A_{1,8}, \quad A_{4,9} = -A_{1,9}, \quad A_{4,10} = A_{1,10}, \quad A_{4,11} = -A_{1,11}\\
A_{5,5} &= 3J_{\mathrm{CH}}(\omega_{\mathrm{H}} + \omega_{\mathrm{C}}) + \frac{1}{2}J_{\mathrm{CH}}(\omega_{\mathrm{H}} - \omega_{\mathrm{C}}) + 6J_{\mathrm{HH}}(2\omega_{\mathrm{H}}) + 3J_{\mathrm{HHH}}(\omega_{\mathrm{H}})\\
&\quad + 3J_{\mathrm{HH}}(\omega_{\mathrm{H}}) + \frac{3}{2}J_{\mathrm{CH}}(\omega_{\mathrm{H}}) + \frac{3}{2}rf_{\mathrm{H}}\\
A_{5,6} &= \frac{1}{\sqrt{3}}(-A_{5,5} + 12J_{\mathrm{HH}}(2\omega_{\mathrm{H}})), \quad A_{5,7} = 0\\
A_{5,8} &= -\sqrt{3}\left(\frac{1}{3}J_{\mathrm{HCH}}(\omega_{\mathrm{H}} - \omega_{\mathrm{C}}) - 2J_{\mathrm{HHH}}(2\omega_{\mathrm{H}}) + \frac{3}{2}J_{\mathrm{HHH}}(\omega_{\mathrm{H}}) + \frac{1}{2}J_{\mathrm{HH}}(\omega_{\mathrm{H}})\right.\\
&\quad \left. + \frac{1}{2}J_{\mathrm{HCH}}(\omega_{\mathrm{H}}) + J_{\mathrm{CHHH}}(\omega_{\mathrm{H}}) + J_{\mathrm{CHH}}(\omega_{\mathrm{H}}) + \frac{1}{2}rf_{\mathrm{H}}\right), \quad A_{5,9} = 0\\
A_{5,10} &= A_{5,8} - \sqrt{3}\left(2J_{\mathrm{HCH}}(\omega_{\mathrm{H}} + \omega_{\mathrm{C}}) - \frac{1}{3}J_{\mathrm{HCH}}(\omega_{\mathrm{H}} - \omega_{\mathrm{C}}) - 2J_{\mathrm{CHHH}}(\omega_{\mathrm{H}}) - 2J_{\mathrm{CHH}}(\omega_{\mathrm{H}})\right)\\
A_{5,11} &= 0, \quad A_{6,6} = \frac{5}{3}A_{5,5} - 8J_{\mathrm{HH}}(2\omega_{\mathrm{H}}) - 8J_{\mathrm{HHH}}(\omega_{\mathrm{H}}), \quad A_{6,7} = 0\\
A_{6,8} &= 4J_{\mathrm{HCH}}(\omega_{\mathrm{H}} + \omega_{\mathrm{C}}) + \frac{1}{3}J_{\mathrm{HCH}}(\omega_{\mathrm{H}} - \omega_{\mathrm{C}}) + 2J_{\mathrm{HHH}}(2\omega_{\mathrm{H}}) + \frac{1}{2}J_{\mathrm{HHH}}(\omega_{\mathrm{H}})\\
&\quad + \frac{3}{2}J_{\mathrm{HH}}(\omega_{\mathrm{H}}) + \frac{3}{2}J_{\mathrm{HCH}}(\omega_{\mathrm{H}}) + 3J_{\mathrm{CHHH}}(\omega_{\mathrm{H}}) - J_{\mathrm{CHH}}(\omega_{\mathrm{H}}) + \frac{3}{2}rf_{\mathrm{H}}, \quad A_{6,9} = 0\\
A_{6,10} &= A_{6,8} - 2J_{\mathrm{HCH}}(\omega_{\mathrm{H}} + \omega_{\mathrm{C}}) + \frac{1}{3}J_{\mathrm{HCH}}(\omega_{\mathrm{H}} - \omega_{\mathrm{C}}) - 6J_{\mathrm{CHHH}}(\omega_{\mathrm{H}}) + 2J_{\mathrm{CHH}}(\omega_{\mathrm{H}})\\
A_{6,11} &= 0, \quad A_{7,7} = \frac{4}{3}A_{5,5}, \quad A_{7,8} = 0\\
A_{7,9} &= \frac{2}{3}J_{\mathrm{HCH}}(\omega_{\mathrm{H}} - \omega_{\mathrm{C}}) + 4J_{\mathrm{HHH}}(2\omega_{\mathrm{H}}) + 3J_{\mathrm{HHH}}(\omega_{\mathrm{H}}) + J_{\mathrm{HH}}(\omega_{\mathrm{H}})\\
&\quad + J_{\mathrm{HCH}}(\omega_{\mathrm{H}}) + 2J_{\mathrm{CHHH}}(\omega_{\mathrm{H}}) + 2J_{\mathrm{CHH}}(\omega_{\mathrm{H}}) + rf_{\mathrm{H}}, \quad A_{7,10} = 0\\
A_{7,11} &= A_{7,9} + 4J_{\mathrm{HCH}}(\omega_{\mathrm{H}} + \omega_{\mathrm{C}}) - \frac{2}{3}J_{\mathrm{HCH}}(\omega_{\mathrm{H}} - \omega_{\mathrm{C}}) - 4J_{\mathrm{CHHH}}(\omega_{\mathrm{H}}) - 4J_{\mathrm{CHH}}(\omega_{\mathrm{H}})\\
A_{8,8} &= 6J_{\mathrm{HCH}}(\omega_{\mathrm{H}} + \omega_{\mathrm{C}}) + 6J_{\mathrm{CH}}(\omega_{\mathrm{H}} + \omega_{\mathrm{C}}) + \frac{1}{3}J_{\mathrm{HCH}}(\omega_{\mathrm{H}} - \omega_{\mathrm{C}}) + \frac{1}{3}J_{\mathrm{CH}}(\omega_{\mathrm{H}} - \omega_{\mathrm{C}})\\
&\quad + 2J_{\mathrm{HHH}}(2\omega_{\mathrm{H}}) + 2J_{\mathrm{HH}}(2\omega_{\mathrm{H}}) + 4J_{\mathrm{HH}}(\omega_{\mathrm{H}}) + J_{\mathrm{HCH}}(\omega_{\mathrm{H}}) + 2J_{\mathrm{CHHH}}(\omega_{\mathrm{H}})\\
&\quad + 2J_{\mathrm{CHH}}(\omega_{\mathrm{H}}) + \frac{3}{2}J_{\mathrm{CH}}(\omega_{\mathrm{H}}) + \frac{5}{2}rf_{\mathrm{H}} - J_{\mathrm{HCH}}(\omega_{\mathrm{C}}) + \frac{3}{2}J_{\mathrm{CH}}(\omega_{\mathrm{C}}) + \frac{1}{2}rf_{\mathrm{C}} - 3J_{\mathrm{HHH}}(0)\\
&\quad + 3J_{\mathrm{HH}}(0) - \frac{4}{3}J_{\mathrm{HCH}}(0) - 4J_{\mathrm{CHHH}}(0) + 4J_{\mathrm{CHH}}(0) + \frac{4}{3}J_{\mathrm{CH}}(0), \quad A_{8,9} = 0\\
A_{8,10} &= 2J_{\mathrm{HHH}}(\omega_{\mathrm{H}}) - 2J_{\mathrm{HH}}(\omega_{\mathrm{H}}) + J_{\mathrm{HCH}}(\omega_{\mathrm{H}}) + \frac{1}{2}J_{\mathrm{CH}}(\omega_{\mathrm{H}}) + \frac{3}{2}rf_{\mathrm{H}}\\
&\quad - J_{\mathrm{HCH}}(\omega_{\mathrm{C}}) + \frac{1}{2}J_{\mathrm{CH}}(\omega_{\mathrm{C}}) - \frac{1}{2}rf_{\mathrm{C}}\\
A_{8,11} &= 0, \quad A_{9,9} = A_{8,8} - 8J_{\mathrm{HCH}}(\omega_{\mathrm{H}} + \omega_{\mathrm{C}}) - 4J_{\mathrm{CH}}(\omega_{\mathrm{H}} + \omega_{\mathrm{C}}), \quad A_{9,10} = 0\\
A_{9,11} &= -2J_{\mathrm{HHH}}(\omega_{\mathrm{H}}) + 2J_{\mathrm{HH}}(\omega_{\mathrm{H}}) - J_{\mathrm{HCH}}(\omega_{\mathrm{H}}) - \frac{1}{2}J_{\mathrm{CH}}(\omega_{\mathrm{H}}) - \frac{3}{2}rf_{\mathrm{H}}\\
&\quad - J_{\mathrm{HCH}}(\omega_{\mathrm{C}}) + \frac{1}{2}J_{\mathrm{CH}}(\omega_{\mathrm{C}}) - \frac{1}{2}rf_{\mathrm{C}}\\
A_{10,10} &= A_{8,8} - 4J_{\mathrm{HCH}}(\omega_{\mathrm{H}} + \omega_{\mathrm{C}}) - 4J_{\mathrm{CH}}(\omega_{\mathrm{H}} + \omega_{\mathrm{C}}) + \frac{2}{3}J_{\mathrm{HCH}}(\omega_{\mathrm{H}} - \omega_{\mathrm{C}})\\
&\quad + \frac{2}{3}J_{\mathrm{CH}}(\omega_{\mathrm{H}} - \omega_{\mathrm{C}}) - 4J_{\mathrm{CHHH}}(\omega_{\mathrm{H}}) - 4J_{\mathrm{CHH}}(\omega_{\mathrm{H}}) + 8J_{\mathrm{CHHH}}(0) - 8J_{\mathrm{CHH}}(0)\\
A_{10,11} &= 0, \quad A_{11,11} = A_{10,10} - \frac{4}{3}J_{\mathrm{HCH}}(\omega_{\mathrm{H}} - \omega_{\mathrm{C}}) - \frac{2}{3}J_{\mathrm{CH}}(\omega_{\mathrm{H}} - \omega_{\mathrm{C}})
\end{aligned}
\tag{17}
$$

Like in the previous section, some elements of A matrix are expressed using other elements to simplify the formulas. A large number of elements of the A matrix are zero or just proportional to other elements. This is because the starting matrix R contains some symmetries, for example among the 1600 (40×40) elements for the CH_3 group only 24 are distinct [10]. However, we did not consider any symmetries in our symbolic calculations, because the evaluation of all the 1600 elements takes only around 30 seconds on a desktop computer using our home-written Maxima script.

Assuming the symmetric top diffusional motion for CH_3I, the J's can be given as [10]:

$$J_{\underset{(HH)}{CH}}(\omega) = \frac{3}{40}\left(\frac{\mu_0\gamma_H\gamma_{\underset{(H)}{C}}\hbar}{4\pi r^3_{\underset{(HH)}{CH}}}\right)^2 \times \left[\left(3\cos^2\theta_{\underset{(HH)}{CH}} - 1\right)^2 \frac{6D_\perp}{(6D_\perp)^2+\omega^2} + 12\cos^2\theta_{\underset{(HH)}{CH}}\sin^2\theta_{\underset{(HH)}{CH}} \frac{5D_\perp + D_\parallel}{(5D_\perp + D_\parallel)^2+\omega^2} + 3\sin^4\theta_{\underset{(HH)}{CH}} \frac{2D_\perp + 4D_\parallel}{(2D_\perp + 4D_\parallel)^2+\omega^2}\right] \quad (18)$$

$$J_{\underset{(CHH)}{HCH}}(\omega) = \frac{3}{40}\left(\frac{\mu_0\hbar}{4\pi}\right)^2 \frac{\gamma_H^2\gamma_C\gamma_{\underset{(H)}{C}}}{r^3_{CH}r^3_{\underset{(HH)}{CH}}} \times \left[(3\cos^2\theta_{CH} - 1)(3\cos^2\theta_{CH} - 1)\frac{6D_\perp}{(6D_\perp)^2+\omega^2} + 12\cos\theta_{CH}\sin\theta_{CH}\cos\theta_{\underset{(HH)}{CH}}\sin\theta_{\underset{(HH)}{CH}} \times \cos\left(\varphi_{CH} - \varphi_{\underset{(HH)}{CH'}}\right) \times \frac{5D_\perp + D_\parallel}{(5D_\perp + D_\parallel)^2+\omega^2} + 3\sin^2\theta_{CH}\sin^2\theta_{\underset{(HH)}{CH}} \times \cos\left(2\varphi_{CH} - 2\varphi_{\underset{(HH)}{CH'}}\right)\frac{2D_\perp + 4D_\parallel}{(2D_\perp + 4D_\parallel)^2+\omega^2}\right] \quad (19)$$

$$J_{\underset{(HHH)}{CHHH}}(\omega) = \frac{3}{40}\left(\frac{\mu_0\hbar}{4\pi}\right)^2 \frac{\gamma_H^3\gamma_{\underset{(H)}{C}}}{r^3_{HH}r^3_{\underset{(HH)}{CH}}} \times \left[\left(3\cos^2\theta_{\underset{(HH)}{CH}} - 1\right)(3\cos^2\theta_{HH} - 1)\frac{6D_\perp}{(6D_\perp)^2+\omega^2} + 12\cos\theta_{HH}\sin\theta_{HH}\cos\theta_{\underset{(HH)}{CH}}\sin\theta_{\underset{(HH)}{CH}} \times \cos\left(\varphi_{HH'} - \varphi_{\underset{(HH'')}{CH''}}\right)\frac{5D_\perp + D_\parallel}{(5D_\perp + D_\parallel)^2+\omega^2} + 3\sin^2\theta_{HH} \times \sin^2\theta_{\underset{(HH)}{CH}} \times \cos\left(2\varphi_{HH'} - 2\varphi_{\underset{(HH'')}{CH''}}\right)\frac{2D_\perp + 4D_\parallel}{(2D_\perp + 4D_\parallel)^2+\omega^2}\right] \quad (20)$$

where θ is a polar angle (for tetrahedral geometry $\theta = 109.47^\circ$), and φ is an azimuthal angle. $D_\perp$ and $D_\parallel$ are the rotational diffusion constants. A complete geometrical picture is shown in Fig. 3 of Ref. [10].

3. Experimental

Carbon-13 methyl iodide ($^{13}CH_3I$; 99 at.%, delivered by Eurisotop) was dissolved in deuterated chloroform ($CDCl_3$; 99.8 at.%, MSD isotopes) so that the concentration was 10 mol.%. The solution was transferred to a 5-mm Wilmad NMR tube which was attached to a vacuum line for degassing. After degassing the tube was sealed with a flame.

^{13}C NOESY experiments were carried out on a Bruker DPX200 spectrometer (^{13}C frequency 50.32 MHz) using a 5-mm BBI gradient probe head. Temperature was kept fixed at 300 K. Four scans were accumulated for each mixing time, the relaxation delay being 53 s. A 90° pulse (12.18 μs) was applied, and 8 k and 128 points were collected in the direct and indirect dimensions, respectively, the frequency window being 11 ppm × 11 ppm. Altogether 19 mixing times extending from 3 ms to 45 s were applied.

Intensities of the peaks were determined with the aid of Sparky program [43].

4. Results and discussion

4.1. The appearance of the ^{13}C NOESY spectra

The proton-coupled ^{13}C NOESY for the methyl carbon of methyl iodide consists, at a very short mixing time, of four diagonal peaks corresponding to the four components of the quartet in the 1D ^{13}C spectrum. For longer mixing times, the off-diagonal peaks within the multiplet build up and decay. The spectra at the mixing times of 50 ms, 300 ms and 5000 ms are shown in Fig. 3.

The intensities of the 16 peaks correspond to the elements of the S-matrix in Eq. (8). The 2D peak definitions used in this section are shown in Fig. 4. The diagonal in Figs. 3 and 4 goes from upper left corner to the lower right one (unlike in a usual 2D spectrum) to be in consistence with the mathematical matrix representation. Only the upper right part is depicted in Fig. 4, because the matrix S, like A, is symmetric. As a result of negligible CSA relaxation (see below), the S matrix is in fact symmetric with respect to both diagonals, and in consequence there are only six independent signals (as shown in Fig. 4).

The experimental intensities were analyzed using a program written in Fortran, which allows both simulations and data fitting. Lapack [44] routines are used for diagonalization of the A matrix. The possible fitting parameters are: a scaling factor (needed because experimental intensities are reported in arbitrary units), the C–H bond length, θ_{CH} (the angle between the three-fold symmetry axis and the C–H vector), the rotational diffusion coefficients

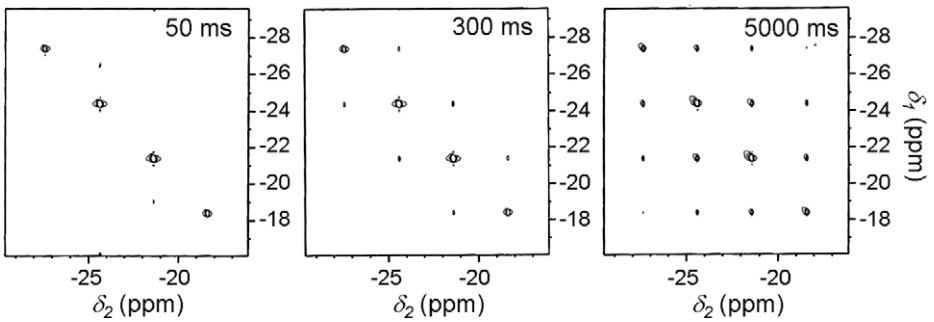

Fig. 3. 2D NOESY spectra of methyl iodide collected at different mixing times (50 ms, 300 ms, and 5000 ms).

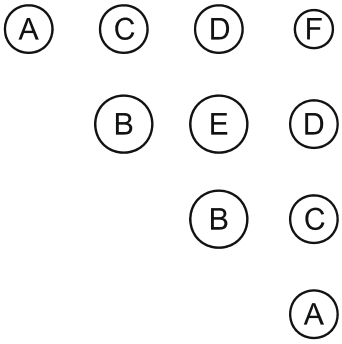

Fig. 4. 2D spectrum signals notation.

$D_{\|}$, $D_{\perp}$, and the random field rates for protons and for the carbon-13 spin (a total of seven parameters). The input file contains intensities of all the distinct lines (A, B, C, D, E, and F; see Fig. 4) for each mixing time, which are obtained by averaging corresponding experimental values. Because different lines have different intensities, and the signal-to-noise ratio is high, the statistical weight of different lines was kept approximately constant.

The ground state geometry of methyl iodide determined from the rotational constants is: $r_{CH} = 1.088$ Å, $r_{CI} = 2.142$ Å, $\alpha_{HCH} = 111°31'$ [45]. The corresponding θ_{CH} is 107.34°. We used this value of θ_{CH} and $r_{CH} = 1.11$ Å (increased by around 2% in order to account for vibrational effects [46,47]) during the data fitting. The simultaneous fitting of build-up/decay for all the six lines, keeping r_{C-H} and θ_{CH} fixed, produced the results shown in Table 1.

It is interesting to note that it is possible to determine directly both rotational diffusion constants with a good accuracy using the NOESY method. Previous attempts, when conventional R_1 and NOE measurements were used, allowed only for the determination of an effective correlation time τ_{eff} for the C–H bond (e.g. [29]). The coefficients $D_{\|}$ and $D_{\perp}$ were then estimated using different models, and the resulting τ_{eff} was compared with experimental one [29]. When the NOESY method is used, however, the different spectral densities (especially the cross-correlated ones) provide much more geometry-specific information.

As $D_{\|}$ is 10 times larger then $D_{\perp}$, the rotational motion of methyl iodide is strongly anisotropic (as was expected). Quite similar values were reported previously [29]. Correlation times calculated from the diffusion constants are very short: $\tau_{\|} = 0.083$ ps, and $\tau_{\perp} = 0.88$ ps. Thus, the rotational motion of methyl iodide molecules is very fast, and partly outside of the diffusional range [48]. Assuming the C–H bond length to be 1.1 Å, the pure inertial rotational correlation times at 300 K are: $\tau_{\|} = 0.068$ ps, and $\tau_{\perp} = 0.32$ ps. It means that the rotational motion around the symmetry axis is in the inertial regime, and even the tumbling motion is partly outside of the diffusional range. In this regime, equations for spectral densities become more complicated, with three distinct correlation times replacing the two diffusion coefficients [49]. However, we found that introducing an additional parameter does not give any noticeable improvement in the fitting. Thus, we decided to use unmodified Eqs. (18)–(20).

Using obtained $D_{\|}$ and $D_{\perp}$, the pure dipole–dipole ^{13}C $R_{1,DD}$ can be estimated to be 0.016 s^{-1}. Therefore, the "random field" mechanism (arising mainly because of spin-rotation relaxation) is dominant (compare $R^{theor}_{1,rf} = 0.068\,s^{-1}$ with $R^{theor}_{1,DD} = 0.016\,s^{-1}$ for the ^{13}C nucleus). From these data we obtain $R^{theor}_{1,tot} = 0.084\,s^{-1}$ ($T^{theor}_{1,tot} = 11.9$ s), and $\eta^{theor} = 0.38$, while our experimental values are: $T^{exp}_{1,tot} = 11.6 \pm 0.5$ s and $\eta^{exp} = 0.39 \pm 0.05$, therefore our results, obtained from NOESY experiments, are confirmed independently. It is worth noting, that the amount of data obtained using the NOESY approach, together with conventional relaxation parameters, may be sufficient for determination of some structural parameters. For example, fixing θ_{CH} at tetrahedral angle value, 109.5°, will result in $D_{\|} = 3.0 \times 10^{12}$ Hz, while $D_{\perp}$ remains unchanged. Consequently, in this case $R^{theor}_{1,DD} = 0.013\,s^{-1}$, $R^{theor}_{1,rf} = 0.072\,s^{-1}$ ($T^{theor}_{1,tot} = 11.8$ s), and, finally, $\eta^{theor} = 0.30$ is obtained, evidencing worse agreement of predicted η with the experimental value.

Theoretical and experimental peak intensity profiles are compared in Fig. 5. The blue lines correspond to the experimental, and the red ones to the theoretical intensities. The agreement between the two sets of curves is very good.

4.2. The role of the chemical shielding anisotropy relaxation

The CSA interaction is a rank-two interaction, in analogy with the dipole–dipole case, and thus cannot be treated phenomenologically as the spin-rotation (rank one) interaction. If the CSA–dipole–dipole cross-correlations are small, there is no need to complicate the treatment, which would require a consideration of new parameters. Contrary to the conclusions of Simcox et al. [29], two kinds of independent evidence can be given to show that the rate of the CSA auto relaxation is negligible at 4.7 T magnetic field. The value of chemical shielding anisotropy of the ^{13}C nucleus in CH_3I is around −40 ppm, as obtained recently from liquid crystal measurements [50], and quantum chemical calculations [51]. Because of the symmetry of the molecule, the unique axis of the ^{13}C CSA tensor coincides with the C_3 axis and the CSA relaxation rate depends only on the tumbling reorientation rate. Assuming $\Delta\sigma = -40$ ppm, $B_0 = 4.7$ T, and $D_{\perp} = 1.9 \times 10^{11}$ Hz (see Table 1 above), the CSA contribution to the spin-lattice relaxation rate, $R_{1,CSA} = 1.9 \times 10^{-5}\,s^{-1}$ is obtained, which is more than 800 times slower than $R_{1,DD} = 0.016\,s^{-1}$. However, the CSA–dipole–dipole CCRR will not be so small, because while $R_{1,DD}$ and $R_{1,CSA}$ are proportional to the appropriate squared interaction strength constants,

Table 1
Fitted parameters and their uncertainties for iodomethane in chloroform solution

Parameter	Value
Scaling factor	87.57 ± 0.17
r_{CH} (Å)	1.11
θ (°)	107.34
$D_{\|}$(Hz)	$2.0 \times 10^{12} \pm 0.3 \times 10^{12}$
$D_{\perp}$(Hz)	$1.9 \times 10^{11} \pm 0.2 \times 10^{11}$
rf_H (s^{-1})	0.121 ± 0.001
rf_C (s^{-1})	0.068 ± 0.002

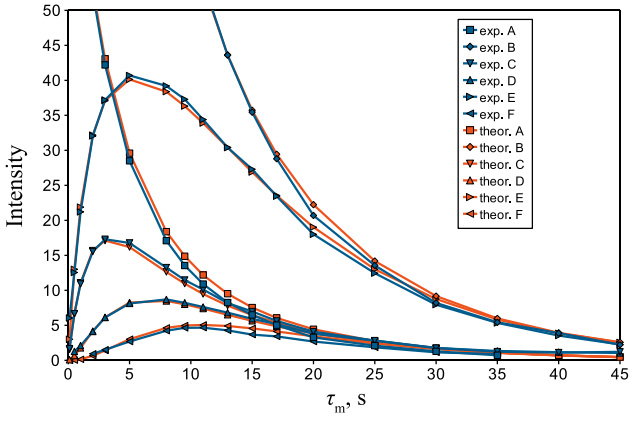

Fig. 5. Comparison of experimental (blue) and theoretical (red) intensity profiles. Points are connected by straight lines for convenience. For the lines labeling convention see Fig. 4.

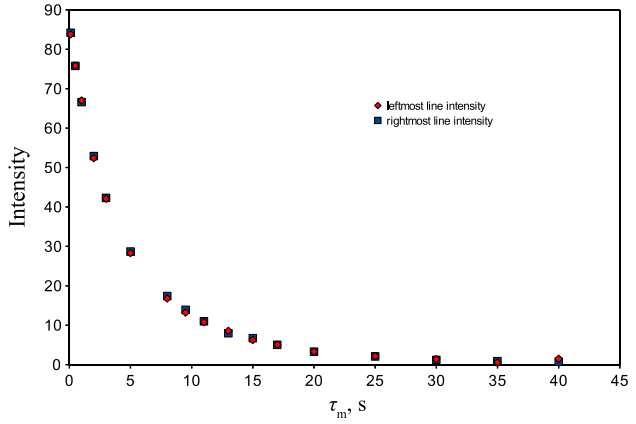

Fig. 6. Time dependence of the diagonal line intensities in NOESY experiment.

the cross-correlated Γ_{DD-CSA} rate is proportional to the dipole–dipole coupling constant and $\gamma_{^{13}C}\Delta\sigma B_0$. In the case of small $\Delta\sigma$, the CCRR attains a much higher value than the $R_{1,CSA}$ [2,21]. For example, Γ^{long}_{DD-CSA} can be roughly (omitting geometrical relations) estimated to be around $1/\left(1+\sqrt{800}\right) \approx 0.034(3.4\%)$ of the dipole–dipole auto relaxation rate, which is not completely negligible. Yet, the inspection of the intensities of the outermost diagonal signals of the ^{13}C quartet shows that the left- and right-most intensities are indistinguishable. This means that we see no evidence of the CSA–DD cross-correlation, probably partly due to the masking by a large spin-rotation contribution (Fig. 6).

5. Conclusions

The relevant theory for the signal intensities in proton-coupled carbon-13 NOESY experiments was derived for degenerate spin systems such as $^{13}CH_2$ and $^{13}CH_3$ groups. It was demonstrated, on a sample of carbon-13 enriched methyl iodide dissolved in chloroform, that the corresponding experiments with variable mixing times can be interpreted quantitatively, and yield relevant information on anisotropic reorientation of small molecules, even in a case where the random field (spin-rotation) relaxation mechanism is very important.

The method might be a general tool for analyzing the effects of the environment on the dynamics of small molecules. We believe that it would work even better in a more viscous system, where the dipole–dipole relaxation plays a larger role, and could probably also be applied for studying liquid–crystalline solutions. Whether it could also be useful for investigations of isolated methyl groups in larger molecules is an open question.

Acknowledgments

This work was supported by the Swedish Research Council, the Carl Trygger's Foundation and the Magn Bergwall's Foundation. V.-V. T. and J.J. are grateful to the Academy of Finland (Grants 123847 and 116824, respectively) for financial support. P.T. acknowledges the grants from the Research Foundation of Orion Corporation, the Tauno Tönning Foundation, the Alfred Kordelin Foundation and the Magnus Ehrnrooth Foundation. E.P. is grateful to the Swedish Institute for financial support.

References

[1] G.C. Levy, D.J. Kerwood, Carbon-13 relaxation measurements: organic chemistry applications, in: D.M. Grant, R.K. Harris (Eds.), Encyclopedia of Nuclear Magnetic Resonance, Wiley, Chichester, 1996, pp. 1147–1157.
[2] J. Kowalewski, L. Mäler, Nuclear Spin Relaxation in Liquids, Taylor and Francis, New York, 2006.
[3] J. Brondeau, D. Canet, Longitudinal magnetic relaxation of ^{13}C (or ^{15}N) interacting with a strongly irradiated proton system, J. Chem. Phys. 67 (1977) 3650–3654.
[4] L.G. Werbelow, D.M. Grant, Proton-decoupled carbon-13 relaxation in $^{13}CH_2$ and $^{13}CH_3$ spin systems, J. Chem. Phys. 63 (1975) 4742–4749.
[5] L.G. Werbelow, D.M. Grant, Intramolecular dipolar relaxation in multispin systems, Adv. Magn. Reson. 9 (1977) 189–299.
[6] D.M. Grant, C.L. Mayne, F. Liu, T.X. Xiang, Spin lattice relaxation of coupled nuclear spins with applications to molecular motion in liquids, Chem. Rev. 91 (1991) 1591–1624.
[7] D.M. Grant, R.A. Brown, Relaxation of coupled spins from rotational diffusion, in: D.M. Grant, R.K. Harris (Eds.), Encyclopedia of Nuclear Magnetic Resonance, Wiley, Chichester, 1996, pp. 4003–4018.
[8] C.L. Mayne, S.A. Smith, Relaxation processes in coupled-spin systems, in: D.M. Grant, R.K. Harris (Eds.), Encyclopedia of Nuclear Magnetic Resonance, Wiley, Chichester, 1996, pp. 4053–4071.
[9] D. Canet, Construction, evolution and detection of magnetization modes designed for treating longitudinal relaxation of weakly coupled spin 1/2 systems with magnetic equivalence, Prog. NMR Spectrosc. 21 (1989) 237–291.
[10] L.G. Werbelow, D.M. Grant, Carbon-13 relaxation in multispin systems of the type AX_n, J. Chem. Phys. 63 (1975) 544–556.
[11] M.T. Chenon, R. Dunkel, D.M. Grant, L.G. Werbelow, NMR relaxation studies of the (CH_3)–C-13 spin grouping in the vicinity of the T1 minimum, J. Phys. Chem. A 103 (1999) 1447–1456.
[12] M.T. Chenon, L.G. Werbelow, An NMR study of the solution dynamics of deltorphin-I, J. Am. Chem. Soc. 124 (2002) 14066–14074.
[13] C. Kim, A.W. Lee, A study on the effect of neighboring protons in proton-coupled spin-lattice relaxation of methylene carbon-13 in *n*-undecane, Bull. Kor. Chem. Soc. 23 (2002) 727–735.
[14] L. Sturz, A. Dölle, Anisotropic reorientational dynamics of toluene in neat liquid. A C-13 nuclear magnetic relaxation study, J. Phys. Chem. A 105 (2001) 5055–5060.
[15] K.E. Kövér, G. Batta, J. Kowalewski, L. Ghalebani, D. Kruk, Internal dynamics of hydroxymethyl rotation from CH_2 cross-correlated dipolar relaxation in methyl-beta-D-glucopyranoside, J. Magn. Reson. 167 (2004) 273–281.
[16] L. Ghalebani, P. Bernatowicz, S.N. Aski, J. Kowalewski, Cross-correlated and conventional dipolar carbon-13 relaxation in methylene groups in small, symmetric molecules, Concepts Magn. Reson. A 30A (2007) 100–115.
[17] L. Ghalebani, D. Kotsyubynskyy, J. Kowalewski, NMR relaxation interference effects and internal dynamics in gamma-cyclodextrin, J. Magn. Reson. 195 (2008) 1–8.
[18] M. Zerbetto, A. Polimeno, D. Kotsyubynskyy, L. Ghalebani, J. Kowalewski, E. Meirovitch, U. Olsson, G. Widmalm, An integrated approach to NMR spin relaxation in flexible biomolecules: application to $\beta-d-$glucopyranosyl $-(1\rightarrow 6)-\alpha-d-$mannopyranosyl-OMe, J. Chem. Phys. 131 (2009) 234501.
[19] A. Kumar, R.C.R. Grace, P.K. Madhu, Cross-correlations in NMR, Prog. NMR Spectrosc. 37 (2000) 191–319.
[20] L. Di Bari, J. Kowalewski, G. Bodenhausen, Magnetization transfer modes in scalar-coupled spin systems investigated by selective 2-dimensional nuclear magnetic resonance exchange experiments, J. Chem. Phys. 93 (1990) 7698–7705.
[21] L. Mäler, J. Kowalewski, Cross-correlation effects in the longitudinal relaxation of heteronuclear spin systems, Chem. Phys. Lett. 192 (1992) 595–600.
[22] Y. Huang, G. Bodenhausen, R.R. Ernst, Use of spy nuclei for relaxation studies in nuclear magnetic resonance, J. Am. Chem. Soc. 103 (1981) 6988–6989.
[23] H. Oschkinat, A. Pastore, G. Bodenhausen, Determination of relaxation pathways in coupled spin systems by two-dimensional NMR exchange spectroscopy with small flip angles, J. Am. Chem. Soc. 109 (1987) 4110–4111.
[24] H. Oschkinat, D. Limat, L. Emsley, G. Bodenhausen, Longitudinal relaxation pathways in scalar-coupled systems, J. Magn. Reson. 81 (1989) 13–42.
[25] J.R. Lyerla Jr., D.M. Grant, R.D. Bertrand, Field-dependent contributions to carbon-13 nuclear relaxation, J. Phys. Chem. 75 (1971) 3967–3971.
[26] K.T. Gillen, M. Schwartz, J.H. Noggle, NMR relaxation time studies in liquid methyl iodide, Mol. Phys. 20 (1971) 899–912.
[27] T.C. Farrar, S.J. Druck, R.R. Shoup, E.D. Becker, Temperature-dependent ^{13}C relaxation studies of small molecules, J. Am. Chem. Soc. 94 (1972) 699–703.
[28] M. Schwartz, ^{13}C relaxation and extended diffusion in prolate symmetric-top molecules, Chem. Phys. Lett. 73 (1980) 127–130.
[29] P.B. Simcox, L.E. Nance, A.A. Rodriguez, Temperature and field dependent ^{13}C NMR relaxation studies of the reorientation of methyl iodide, J. Mol. Liq. 59 (1994) 65–81.
[30] A. Abragam, The Principles of Nuclear Magnetism, Oxford University Press, Oxford, 1961.
[31] A.G. Redfield, The theory of relaxation processes, Adv. Magn. Reson. 1 (1965) 1–32.
[32] A.D. Bain, R.M. Lynden-Bell, The relaxation matrices for AX_2 and AX_3 nuclear spin systems, Mol. Phys. 30 (1975) 325–356.
[33] D.E. Woessner, Nuclear spin relaxation in ellipsoids undergoing rotational brownian motion, J. Chem. Phys. 37 (1962) 647–654.
[34] M. Goldman, Formal theory of spin–lattice relaxation, J. Magn. Reson. 149 (2001) 160–187.

[35] V.A. Daragan, K.H. Mayo, Motional model analyses of protein and peptide dynamics using ^{13}C and ^{15}N NMR relaxation, Prog. NMR Spectrosc. 31 (1997) 63–105.
[36] P. Luginbühl, K. Wüthrich, Semi-classical nuclear spin relaxation theory revisited for use with biological macromolecules, Prog. NMR Spectrosc. 40 (2002) 199–247.
[37] R.K. Wangsness, F. Bloch, The dynamical theory of nuclear induction, Phys. Rev. 89 (1953) 728–739.
[38] A. Wokaun, R.R. Ernst, Selective excitation and detection in multilevel spin systems: application of single transition operators, J. Chem. Phys. 67 (1977) 1752–1758.
[39] S.H. Friedberg, A.J. Insel, L.E. Spence, Linear Algebra, Prentice Hall, New Jersey, 1989.
[40] A. Jerschow, MathNMR: Spin and spatial tensor manipulations in Mathematica, J. Magn. Reson. 176 (2005) 7–14.
[41] I. Kuprov, N. Wagner-Rundell, P.J. Hore, Bloch–Redfield–Wangsness theory engine implementation using symbolic processing software, J. Magn. Reson. 184 (2007) 196–206.
[42] Maxima, a Computer Algebra System. Version 5.18.1 (2009). Available from: http://maxima.sourceforge.net/.
[43] T.D. Goddard, D.G. Kneller, SPARKY3, University of California, San Francisco, USA.
[44] E. Anderson, Z. Bai, C. Bischof, S. Blackford, J. Demmel, J. Dongarra, J. Du Croz, A. Greenbaum, S. Hammarling, A. McKenney, D. Sorensen, LAPACK Users' Guide, Society for Industrial and Applied Mathematics, Philadelphia, 1999.
[45] J.L. Duncan, P.D. Mallinson, The infrared spectrum of CHD_2I and the ground state geometry of methyl iodide, J. Mol. Spectrosc. 39 (1971) 471–478.
[46] E.R. Henry, A. Szabo, Influence of vibrational motion on solid state line shapes and NMR relaxation, J. Chem. Phys. 82 (1985) 4753–4761.
[47] J. Kowalewski, M. Effemey, J. Jokisaari, Dipole–dipole coupling constant for a directly bonded CH pair—A carbon-13 relaxation study, J. Magn. Reson. 157 (2002) 171–177.
[48] K.T. Gillen, J.H. Noggle, NMR studies of the rotational diffusion of symmetric top molecules in liquids, J. Chem. Phys. 53 (1970) 801–809.
[49] H.J. Böhm, R.M. Lynden-Bell, P.A. Madden, I.R. McDonald, Molecular motion in a model of liquid acetonitrile, Mol. Phys. 51 (1984) 761–777.
[50] P. Tallavaara, J. Jokisaari, An alternative NMR method to determine nuclear shielding anisotropies for molecules in liquid–crystalline solutions with ^{13}C shielding anisotropy of methyl iodide as an example, Phys. Chem. Chem. Phys. 10 (2008) 1681–1687.
[51] A.M. Kantola, P. Lantto, J. Vaara, J. Jokisaari, Carbon and proton shielding tensors in methyl halides, Phys. Chem. Chem. Phys. (2010), doi:10.1039/b923506.